

# Influence of chromium concentration and particle size on the ESR linewidth of $\text{Al}_2\text{O}_3:\text{Cr}^{3+}$ powders

R. S. DE BIASI, D. C. S. RODRIGUES

*Seção de Engenharia e Ciência dos Materiais, Instituto Militar de Engenharia, Rio de Janeiro, Brasil*

The linewidth of electron spin resonance (ESR) absorption in polycrystalline samples of chromium-doped alumina ( $\text{Al}_2\text{O}_3:\text{Cr}^{3+}$ ) has been investigated as a function of chromium concentration and particle size. The linewidth is found to be directly proportional to chromium concentration and inversely proportional to particle size. The experimental results are consistent with the mechanism of dipolar broadening in diluted solid solutions; the influence of particle size may be attributed to size-dependent fluctuations of the zero-field parameter,  $D$ .

## 1. Introduction

The electron spin resonance (ESR) absorption spectrum of single-crystal, chromium-doped alumina ( $\text{Al}_2\text{O}_3:\text{Cr}^{3+}$ ) has been investigated by several researchers [1-8]. In particular, the experimental dependence of linewidth on chromium concentration has been satisfactorily explained on the basis of Cr-Cr dipolar broadening [6]. In the present work, a similar study is undertaken using powder samples. Besides allowing more accurate control of sample composition and homogeneity, the use of powder samples introduces another experimental variable, particle size, the effect of which may be of interest for technological applications.

The relevant broadening theories are discussed in the following section. The experimental procedure is described in Section 3. Experimental results are presented and discussed in Section 4.

## 2. Theory

### 2.1. Anisotropy broadening

If an ESR line is anisotropic, the linewidth as measured in a powder is broader than in a single crystal, simply because the powder spectrum is a superposition of the spectra of single crystals with different orientations relative to the magnetic field. This effect is called anisotropy broadening.

Although there is no simple relation between the single-crystal linewidth and the powder linewidth, one can derive this relation for each individual case by simulating the powder spectrum from single-crystal data, keeping the single-crystal linewidth as an adjustable parameter. In the case of  $\text{Al}_2\text{O}_3:\text{Cr}^{3+}$ , the simulation is straightforward, for the following reasons: (a) the spin-Hamiltonian parameters are well known, (b) the symmetry is high (axial), (c) the zero-field splitting parameter  $D$  is fairly large, so that the lines are well separated and the angular dependence of the linewidth may be neglected.

The simulation of the ESR spectrum of  $\text{Al}_2\text{O}_3:\text{Cr}^{3+}$  has been carried out following closely the method described by van Veen [9]. Two different lineshapes, Gaussian and Lorentzian, were assumed. The spectra were computed for several values of the single-crystal linewidth,  $\Delta H_{pp}$ , between 2 and 10 mT. A typical result is shown in Fig. 1, which shows: (a) part of a simulated powder spectrum, assuming a Gaussian lineshape, (b) the same, assuming a Lorentzian lineshape, (c) the experimental curve for one of the powder samples (see Section 4).

Comparison of the simulated spectra with the experimental curves showed that the Lorentzian lineshape yielded a very good agreement. The line-

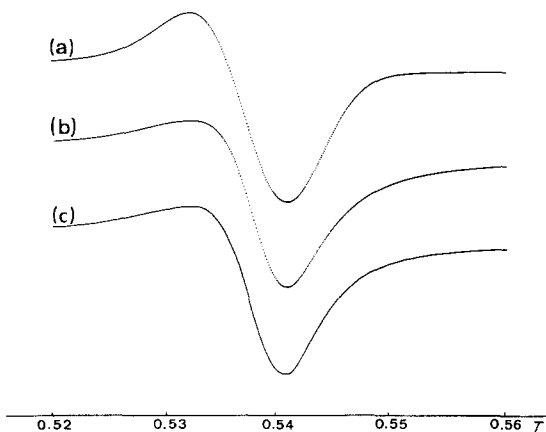


Figure 1 Example of line simulation. (a) Simulated line with  $\Delta H_{pp} = 10$  mT (Gaussian); (b) simulated line with  $\Delta H_{pp} = 6$  mT (Lorentzian); (c) experimental line for a powder sample of a type B alumina doped with 0.2 mol% Cr. The simulated lines have the same powder linewidth as the experimental line. Parameters for lines (a) and (b):  $g_{\parallel} = 1.9817$ ,  $g_{\perp} = 1.9819$ ,  $D = -0.19110$  cm<sup>-1</sup>,  $\nu = 9.50$  GHz.

widths of the powder spectrum were found to be related to the single-crystal linewidths through equations of the form  $\Delta H_{pp}(i)_P = C_i \Delta H_{pp}(i)_{SC}$ , where  $C_i$  is a constant:

$$\Delta H_{pp}(1-2)_P = 1.60 \Delta H_{pp}(1-2)_{SC}; \quad (1)$$

$$\Delta H_{pp}(2-3)_P = 1.20 \Delta H_{pp}(2-3)_{SC}; \quad (2)$$

$$\Delta H_{pp}(3-4)_P = 1.45 \Delta H_{pp}(3-4)_{SC}; \quad (3)$$

where the subscripts P and SC mean powder and single crystal and the transitions are identified in the usual way (see [7]).

## 2.2. Dipolar broadening

According to both the method of moments [10, 11] and the more elaborate theory of Grant and

Strandberg [6], the additional linewidth  $\Delta H_{dd}$  due to dipolar broadening in dilute ( $f < 0.1$  mol%) solid solutions of  $\text{Al}_2\text{O}_3:\text{Cr}^{3+}$  should be a linear function of the chromium concentration  $f$ . The experimental results in single crystals agree with the theoretical predictions (see Fig. 2), although the data show a large spread, especially for higher chromium concentrations. This has been attributed to clustering [6], which is virtually unavoidable when working with single crystals.

## 2.3. Residual linewidth

The residual linewidth, i.e., the linewidth in the limit of vanishing Cr concentration, is of the order of 1.1–1.6 mT in single crystals [5–8], with the magnetic field along the crystal  $c$ -axis. It has been attributed to the hyperfine interactions between the electronic spin of the chromium ions and the spin of the aluminium nuclei [6], plus a small contribution of the mosaic effect and strain broadening, in the so-called “hybrid model” [7]. In the present work, the residual linewidth is taken as an experimental parameter (see Section 4).

## 2.4. Fluctuations of the zero-field splitting parameter

Even when all the preceding mechanisms have been taken into account, there remains the possibility that the zero-field splitting parameter  $D$  may have slightly different values for individual crystal-line sites, due to crystal imperfections. This is seen, for example, in as-cut single crystals, where the surface layer contains dislocations and plastic deformations and is heavily strained. The effect can be minimized through an elaborate procedure of annealing and chemical etching [8].

The influence of fluctuations of the zero-field splitting parameter may be expressed through a

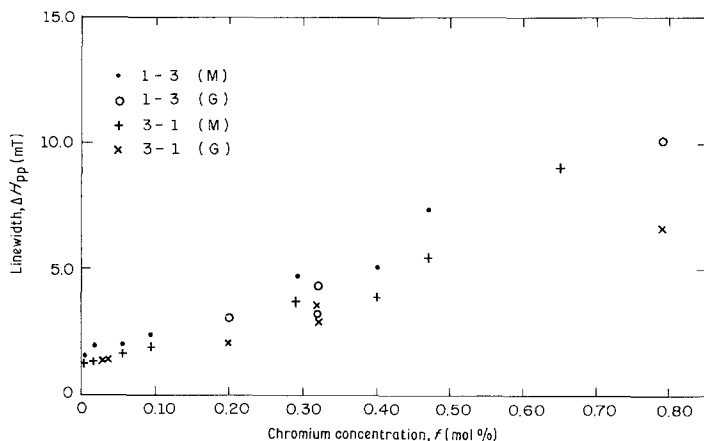


Figure 2 Single-crystal linewidth as a function of chromium concentration. (M): Manenkov and Fedorov [5]; (G): Grant and Standberg [6].

TABLE I Specifications of alumina samples

Type	Particle size ( $\mu\text{m}$ )	Manufacturer
A	0.25	Struers
B	0.80	CBA
C	1.00	Struers
D	6.00	Philips

phenomenological linewidth of the form [9]:

$$\Delta H_D = \sigma \frac{\partial H}{\partial D}, \quad (4)$$

where  $\sigma$  is the standard deviation of the parameter  $D$ . In the case of powder samples, this mechanism is presumably much more important, due to a larger surface-to-volume ratio.

### 2.5. Total broadening

For Lorentzian lineshapes, all the mechanisms above are additive, except anisotropy broadening, which is multiplicative. The resulting powder linewidth may thus be expressed as:

$$\Delta H_{pp}(i) = C_i \left[ \Delta H_0(i) + \Delta H_{dd}(i) + \sigma \frac{\partial H(i)}{\partial D} \right], \quad (5)$$

where  $C_i$  is a constant,  $\Delta H_0$  is the residual linewidth,  $\Delta H_{dd}$  is the additional linewidth due to dipolar broadening and the index  $i$  refers to a particular transition.

### 3. Experimental procedure

The single crystals used in this work were grown by the Czochralski technique and contained about 0.0001 mol% Cr. Powder samples were prepared from pure oxides, carefully grinding them together and then firing the mixture for 96 hours at 1350°C. Four commercial aluminas, with different particle sizes, were used (see Table I). Actual chromium concentrations were determined by X-ray fluorescence spectrometry and particle sizes were checked by transmission electron microscopy. Magnetic resonance measurements were performed at room temperature and 9.5 GHz.

### 4. Experimental results and discussion

Two sets of powder samples were used in the present work: (a) samples with the same particle size, doped with different chromium concentrations and (b) samples with different particle sizes, doped with the same chromium concentration. A typical spectrum is shown in Fig. 3.

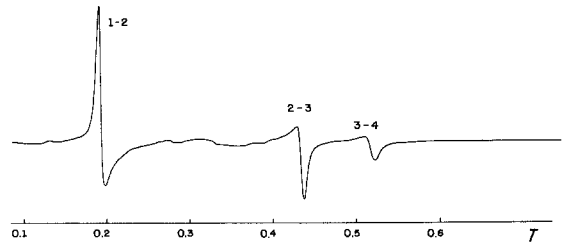


Figure 3 ESR spectrum of a powder sample of Type B alumina doped with 0.53 mol% Cr.

#### 4.1. Influence of chromium concentration

The results for samples prepared from Type B alumina doped with different chromium concentrations are shown in Fig. 4. In the concentration range 0.007–1.15 mol%, the linewidths are accurately described by linear functions of the chromium concentration. The data show a much smaller spread than in single crystals (see Fig 2). Least-square fits yield the following equations:

$$\Delta H_{pp}(1-2) = 3.41 + 7.10f; \quad (6)$$

$$\Delta H_{pp}(2-3) = 4.87 + 6.68f; \quad (7)$$

$$\Delta H_{pp}(3-4) = 6.36 + 10.33f; \quad (8)$$

where  $\Delta H_{pp}$  is in mT and  $f$  in mol%.

#### 4.2. Influence of particle size

The results for samples prepared from aluminas with different particle sizes (Types A–D) and doped with the same chromium concentration (0.1 mol%) are shown in Fig. 5. The linewidths are seen to decrease with increasing particle size. Least-square fits yield the following equations:

$$\Delta H_{pp}(1-2) = 4.56 - 0.08d; \quad (9)$$

$$\Delta H_{pp}(2-3) = 5.78 - 1.89d; \quad (10)$$

$$\Delta H_{pp}(3-4) = 7.89 - 0.24d, \quad (11)$$

where  $\Delta H_{pp}$  is in mT and  $d$  is the particle size in micrometers.

#### 4.3. Residual linewidths

The powder residual linewidths are the concentration-independent terms in Equations 6 to 8. They are much larger than the reported values [5–8] for the single-crystal residual linewidths. These values, however, refer to measurements taken with the magnetic field along the crystal  $c$ -axis, while the linewidths which are relevant to the powder spectrum correspond to the turning points [4, 9] of the spin Hamiltonian ( $90^\circ$  for the

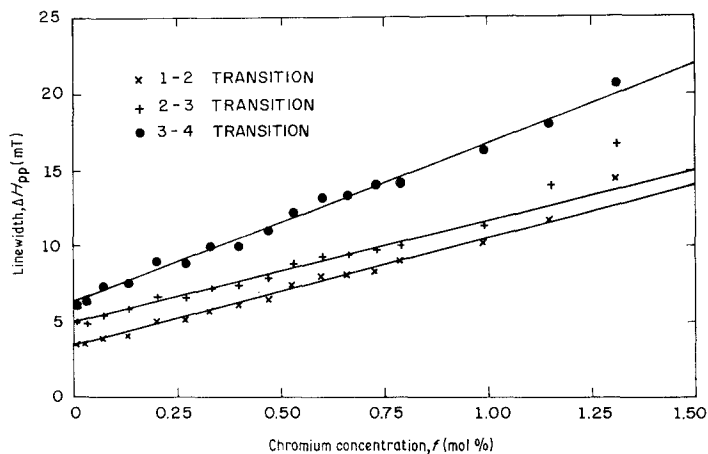


Figure 4 Powder linewidths as functions of chromium concentration. The full lines are least-square fits to the experimental data in the range 0.007–1.15 mol%.

1–2 and 3–4 transitions and 35° for the 2–3 transition). For that reason, we performed careful measurements on slightly doped single crystals oriented along the relevant directions. The measured linewidths, after being corrected for anisotropy broadening, could then be compared with the powder residual linewidths. The results are shown in Table II.

The results in Table II show that the linewidth in powders involves an additional broadening mechanism that is not found in single crystals, or at least is much less important in single crystals. The most probable mechanism is the fluctuation of the zero-field splitting parameter, already discussed in Section 2.

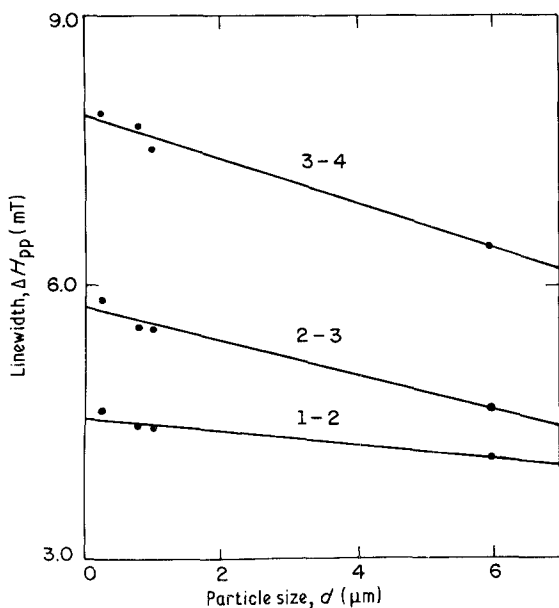


Figure 5 Powder linewidths as functions of particle size. The full lines are least-square fits to the experimental data.

#### 4.4. Discussion

According to Equation 5 and the preceding arguments, the standard deviation of  $D$  is given by:

$$\sigma(i) = \{ \Delta H_{pp}(i) - C_i [\Delta H_0(i) - \Delta H_{dd}(i)] \} / C_i \partial H(i) / \partial D, \quad (12)$$

where the computed value of  $\sigma$  should be the same for all transitions.

The terms on the right-hand side of Equation 12 can be determined in the following way:  $\Delta H_{pp}$ , from Equations 9 to 11;  $C_i$ , from Equations 1 to 3;  $\Delta H_0$ , from single-crystal measurements (see Table II);  $\Delta H_{dd}$ , from Equations 6 to 8, taking  $f = 0.1\%$ ; and  $\partial H(i) / \partial D$ , by computer diagonalization of the spin Hamiltonian. The results are:

$$\sigma(1-2) = 3.5 \times 10^{-3} - 1.9 \times 10^{-4} d; \quad (13)$$

$$\sigma(2-3) = 3.3 \times 10^{-3} - 1.7 \times 10^{-4} d; \quad (14)$$

$$\sigma(3-4) = 3.2 \times 10^{-3} - 1.8 \times 10^{-4} d; \quad (15)$$

where  $\sigma$  is in  $\text{cm}^{-1}$  and  $d$  is in micrometers.

The computed values of  $\sigma$  are close enough to validate our model. Taking the average for the three transitions, an approximate equation for the dependence of  $\sigma$  on particle size is obtained:

$$\sigma = 3.3 \times 10^{-3} - 1.8 \times 10^{-4} d. \quad (16)$$

TABLE II Comparison between intrinsic linewidths in single crystals and powders

Transition	$\Delta H_0$ (mT) single crystal	$C_i$	$\Delta H_0$ (mT) corrected*	$\Delta H_0$ (mT) powder†
1–2	1.50	1.60	2.40	3.41
2–3	1.30	1.20	1.56	4.87
3–4	1.70	1.45	2.47	6.36

\*Using Equations 1 to 3.

†According to Equations 6 to 8.

Of course, Equation 16 holds only for small particle sizes, since  $\sigma$  cannot be negative. Moreover,  $\sigma$  should approach zero gradually, so that the linearity implied by Equation 16 is not expected to hold for large particle sizes. However, Equation 16 can be used to estimate the particle size  $d_{\text{lim}}$  above which  $D$ -fluctuation broadening ceases to be important. Taking  $\sigma = 0$  in Equation 16, gives

$$d_{\text{lim}} = 18 \mu\text{m}.$$

The fact that  $\sigma$  increases with decreasing particle size may be attributed to an increasing surface-to-volume ratio.

## 5. Conclusions

Two main points have been made. First, in the case of  $\text{Al}_2\text{O}_3:\text{Cr}^{3+}$ , meaningful single-crystal linewidth data can be obtained from powder measurements; second, crystallite linewidths are dependent on particle size, so that powder linewidths are not related to chromium concentration in an unambiguous way.

## References

1. A. A. MANENKOV and A. M. PROKHOROV, *Sov. Phys.-JETP* **1** (1955) 611.
2. M. M. ZARIPOV and I. I. SHAMONIN, *ibid.* **3** (1956) 171.
3. J. E. GEUSIC, *Phys. Rev.* **102** (1956) 1252.
4. E. O. SCHULZ-DU BOIS, *Bell Syst. Tech. J.* **38** (1959) 271.
5. A. A. MANENKOV and V. B. FEDOROV, *Sov. Phys.-JETP* **11** (1960) 751.
6. W. J. C. GRANT and M. W. P. STRANDBERG, *Phys. Rev.* **135** (1964) A727.
7. R. F. WENZEL and Y. W. KIM, *ibid.* **140** (1965) A1592.
8. T. T. CHANG, D. FOSTER and A. H. KAHN, *NBS J. Res.* **83** (1978) 133.
9. G. VAN VEEN, *J. Magn. Resonance* **30** (1978) 91.
10. J. H. VAN VLECK, *Phys. Rev.* **74** (1948) 1168.
11. C. KITTEL and E. ABRAHAMS, *ibid.* **90** (1953) 238.

Received 22 May and accepted 4 September 1980.